THE JOURNAL OF BIOLOGICAL CHEMISTRY
Vol. 272, No. 40, Issue of October 3, pp. 25029–25036, 1997

Printed in U.S.A.

The Stathmin/Tubulin Interaction *in Vitro**

(Received for publication, June 26, 1997, and in revised form, July 29, 1997)

Patrick A. Curmi‡§, Søren S. L. Andersen¶, Sylvie Lachkar‡, Olivier Gavet‡, Eric Karsenti¶, Marcel Knossow‖, and André Sobel‡

From ‡INSERM U440, 17 rue du Fer à Moulin, 75005 Paris, France, ¶EMBL, Cell Biology Program, D-69012 Heidelberg, Germany, and ‖Laboratoire d'Enzymologie et Biologie Structurale UPR 9063 CNRS, 91198 Gif sur Yvette, France

Stathmin is a highly conserved ubiquitous cytoplasmic protein, phosphorylated in response to extracellular signals and during the cell cycle. Stathmin has recently been shown to destabilize microtubules, but the molecular mechanisms of this function remained unclear. We show here that stathmin directly interacts with tubulin. We assessed the conditions of this interaction and determined some its quantitative parameters using plasmon resonance, gel filtration chromatography, and analytical ultracentrifugation. The stathmin/tubulin interaction leads to the formation of a 7.7 S complex with a 60-Å Stokes radius, associating one stathmin with two tubulin heterodimer molecules as determined by direct quantification by Western blotting. This interaction is sensitive to pH and ionic environment. Its equilibrium dissociation constant, determined by plasmon resonance measurement of kinetic constants, has an optimum value of 0.5 μM at pH 6.5. The affinity was lowered with a fully "pseudophosphorylated" 4-Glu mutant form of stathmin, suggesting that it is modulated *in vivo* by stathmin phosphorylation. Finally, analysis of microtubule dynamics by video microscopy shows that, in our conditions, stathmin reduces the growth rate of microtubules with no effect on the catastrophe frequency. Overall, our results suggest that the stathmin destabilizing activity on microtubules is related to tubulin sequestration by stathmin.

Stathmin (1, 2), also designated Op18, p18, p19, prosolin, and metablastin (3–6), is a ubiquitous cytosolic phosphoprotein highly conserved in vertebrates (7, 8) and specifically abundant in neurons (9–11). Expression and phosphorylation of stathmin are modulated in various situations related to the control of cellular activities, and it has been proposed that it may act as a relay integrating various intracellular signaling pathways (1). Expression of stathmin was shown to be regulated *in vivo* during development (7, 12–14), during tissue regeneration (15, 16), and in cell culture by cell/cell interactions (17). Stathmin is also up-regulated in many malignant cell types and tumors (5, 18, 19). Phosphorylation of stathmin is observed in response to hormones (20), cytokines (21), neurotransmitters (22), and growth and differentiation factors (23). Moreover, progression through the cell cycle appears to require multisite phosphorylation of stathmin (24). Actually, overexpression of a nonphosphorylatable mutant of stathmin resulted in a large population of cells blocked in G_2/M with a high DNA content (24, 25). Finally, stathmin is the generic element of a protein family whose other members most probably play distinct roles related to the control of neuronal differentiation or to the expression of neuron-specific traits (8, 26).

The molecular mechanism(s) by which stathmin acts in these processes remain largely unknown. Two domains can be distinguished in the primary structure of stathmin, an N-terminal "regulatory" domain that contains the four phosphorylation sites that account for all of the electrophoretic forms of stathmin observed *in vivo* (27) and a C-terminal "interaction" domain that includes a predicted coiled-coil forming α-helical structure thought to interact with other proteins (28). Various stathmin protein partners have been identified in our laboratory (28) including a novel type of protein kinase, KIS (29). Recently, stathmin has been identified as a major microtubule (MT)[1]-destabilizing factor in *Xenopus* egg extracts (30). It was proposed that stathmin binds to unpolymerized tubulin subunits and regulates the dynamic instability of MTs by increasing the frequency of catastrophes. Stathmin also inhibited spontaneous polymerization of tubulin in a substoichiometric fashion. Stathmin is thus the second factor identified that acts as a negative regulator of tubulin polymerization (31). Overexpression of wild type stathmin or of a CDK target site mutant both elicited rapid depolymerization of MTs *in vivo* (32). Horwitz *et al.* (33) showed that, *in vivo*, microinjection of recombinant stathmin induced a loss of MTs in COS-7 cells and, *in vitro*, that stoichiometric amounts of stathmin were able to either prevent assembly or promote disassembly of MTs. Interestingly, this latter result was also noted with the stathmin domain of SCG10, a neuron-specific member of the stathmin family (34). However, the molecular mechanisms by which stathmin destabilizes MTs still remain unclear.

In this study, we assessed quantitatively the conditions of the stathmin/tubulin interaction and determined some of the binding parameters of the interaction, using gel filtration chromatography, plasmon resonance, and analytical ultracentrifugation. Furthermore, we examined the influence of stathmin on the polymerization kinetics of tubulin using video-enhanced contrast, differential interference contrast microscopy. We demonstrate that stathmin interacts directly with tubulin, with a maximum affinity of 0.5 μM around pH 6.5. This interaction leads to formation of a 217-kDa complex consisting of the association of one stathmin with two tubulin heterodimer molecules. Furthermore, we observed that the sole effect of stathmin on MT dynamics in our conditions, as analyzed by video

* This work was supported by funds from the Institut National de la Santé et de la Recherche Médicale, l'Association Française contre les Myopathies, l'Association pour la Recherche contre le Cancer, and the Ligue Nationale Française Contre le Cancer. The costs of publication of this article were defrayed in part by the payment of page charges. This article must therefore be hereby marked "*advertisement*" in accordance with 18 U.S.C. Section 1734 solely to indicate this fact.

§ To whom correspondence should be addressed: INSERM U440, 17 rue du Fer à Moulin, 75005 Paris, France. Tel.: 33 1 45 87 61 30; Fax: 33 1 45 87 61 32; E-mail: curmi@infobiogen.fr.

[1] The abbreviations used are: MT, microtubule; BSA, bovine serum albumin; Fc, flow cell; f_{cat}, catastrophe frequency; R_S, Stokes radius; RU, resonance unit; Vg, growth rate; Pipes, 1,4-piperazinediethanesulfonic acid; WT, recombinant wild type; bWT, boiled recombinant wild type; FPLC, fast protein liquid chromatography.

microscopy, was a reduction of the MT growth rate, independently of any effect on the catastrophe frequency.

EXPERIMENTAL PROCEDURES

Purification of Tubulin and Stathmin—Tubulin was prepared from calf brain by two cycles of polymerization and depolymerization followed by chromatography on phosphocellulose and an additional cycle of polymerization and depolymerization (35). The product was stored at −80 °C at a concentration of 8.2 mg/ml in 20 mM K-Pipes, pH 6.8, 0.25 mM EGTA, 0.25 mM $MgCl_2$, until use.

Recombinant wild type (WT) stathmin, E mutants (16E, 25E, 38E, 25/38E, or 4E in which Ser-16, Ser-25, Ser-38, Ser-25/38, or Ser-16/25/38/63 were, respectively, substituted for Glu) and 4A mutant (Ser-16/25/38/63 substituted for Ala) were prepared as described previously (36). Boiled recombinant wild type (bWT) stathmin was prepared as follows. After sonication of WT stathmin expressing bacteria in extraction buffer, a low speed supernatant was complemented with 100 mM NaCl and heated at 100 °C for 3 min and then ultracentrifuged, and the supernatant was recovered. It was used to purify stathmin to homogeneity in a two-step procedure: anion exchange chromatography and FPLC gel filtration on a Superose 12 HR 10/30 column (Pharmacia, Uppsala, Sweden). Pure stathmin was concentrated to about 20 mg/ml in water on Centriprep-10 (Amicon) and stored at −80 °C. Protein concentrations were achieved by amino acid determination.

Gel Filtration Chromatography—To estimate the Stokes radius (R_S) of tubulin, stathmin, and the stathmin-tubulin complex, proteins were subjected to gel filtration on an FPLC Superose 12 HR 10/30 column. Samples (100 μl) were run on the column after equilibration in AB buffer (80 mM K-Pipes, pH 6.5, 1 mM EGTA, 5 mM $MgCl_2$) at 0.5 ml/min. Standard proteins used to calibrate the column were ribonuclease A (R_S = 16.4 Å), ovalbumin (R_S = 30.5 Å), bovine serum albumin (R_S = 35.5 Å), aldolase (R_S = 48.1 Å), and ferritin (R_S = 61 Å) (gel filtration calibration kit (Pharmacia)). Gel filtration data are presented either as elution volumes or as the molecular sieve coefficient, K_{av}, a parameter calculated as $(V_e - V_0)/(V_t - V_0)$, where V_e represents the elution volume corresponding to the peak concentration of a protein, V_0 is void volume of the column, and V_t is total volume of the gel bed. The void volume was determined by measuring the elution volume with blue dextran. The Stokes radius of the stathmin-tubulin complex was determined graphically on a $(-\log K_{av})^{1/2}$ *versus* Stokes radius plot, according to Siegel and Monty (37), constructed with the above mentioned standard proteins. Spectrophotometer recordings were performed at 280 nm to detect tubulin and the stathmin-tubulin complex, because at this wavelength stathmin is not absorbing (36).

Plasmon Resonance Experiments—BIAcore™ 2000 system, sensor chip CM5, HBS buffer (10 mM HEPES, pH 7.4, 150 mM NaCl, 3.4 mM EDTA, 0.005% (v/v) surfactant p20), and an amine-coupling kit containing *N*-hydroxysuccinimide, *N*-ethyl-*N*′-(3-diethyl-aminopropyl)-carbodiimide, and 1 M ethanolamine-hydrochloride, pH 8.5, were obtained from Pharmacia Biosensor AB (Uppsala, Sweden).

Flow cells (Fc) were prepared with the various stathmin forms: WT, bWT, 16E, 25E, 38E, 25/38E, 4E, and 4A. Immobilization of the different forms of stathmin to the CM5 sensor chip was performed in the BIAcore system as follows. A continuous flow of HBS buffer over the sensor surface at 10 μl/min was maintained. The carboxylated dextran matrix was activated by the injection of 70 μl of a solution containing 0.2 M *N*-ethyl-*N*′-(3-diethyl-aminopropyl)-carbodiimide and 0.05 M *N*-hydroxysuccinimide. Next, 40–80 μl of stathmin (30 μg/ml in 10 mM sodium acetate, pH 5) were injected, followed by 70 μl of ethanolamine to block remaining *N*-hydroxysuccinimide ester groups. The immobilization levels were 1000 resonance units (RU) and 2000 RU for WT, 1000 RU for bWT, 570 RU for 4E, and 1000 RU for 4A. Control flow cells consisted either of an activated-deactivated flow cell or of a flow cell coupled with bovine serum albumin (1000 RU).

To follow the interaction of tubulin with sensor chip-coupled stathmin, an analytical cycle consisted in the injection of 14 μl of tubulin at increasing concentrations (1, 2, 3, 6, 8, 10, and 20 μM) in AB buffer at the indicated pH (pH 6–7.5, with 0.25 pH unit steps) and at a flow rate of 7 μl/min at 25 °C. Analytical cycles were preprogrammed, and the entire analysis was completely automated.

Kinetic Analysis of Plasmon Resonance Results—Interaction curves were obtained, and data were evaluated as shown in Fig. 3. We used the rate equation,

$$dR/dt = k'_a C\,(R_{max} - R_t) - k'_d R_t \qquad \text{(Eq. 1)}$$

assuming a single site interaction between stathmin and tubulin, where dR/dt is the rate of formation of surface complexes (*i.e.* the derivative of the observed response curve), C is the concentration of tubulin (constant), R_{max} is the total amount of immobilized ligand expressed as surface plasmon resonance response, R_t is the response observed at time t, and $R_{max} - R_t$ is the amount of remaining free binding sites at time t. (Please note that all the rate and derived equilibrium constants calculated here are reported with a prime to indicate that they are not solution constants). To calculate the dissociation rate constant, k'_d, data obtained with a high flow of buffer passing over the flow cell (assuming no rebinding) were fitted to the equation,

$$R = R_0 \cdot e^{-k'_d(t - t_0)} \qquad \text{(Eq. 2)}$$

where R is the observed response, R_0 is the response at the start of the dissociation, t is time in seconds, and t_0 is the start time for the dissociation. The association rate constant, k'_a, was then calculated by fitting data to the equation,

$$R = R_{eq}(1 - e^{-(k'_a C_n + k'_d)(t - t_0)}) \qquad \text{(Eq. 3)}$$

where R_{eq} is the steady state response level, C is the molar concentration of tubulin, n is the steric interference factor (default 1, assuming a homogeneous single-site interaction between stathmin and tubulin), t_0 is the start time of association, and k'_d is the dissociation rate constant. The fit was assessed by comparing constants obtained at different tubulin concentrations and by examining the χ^2 and the residual plots for the fitting. A good fit was considered when χ^2 was <1.

Video Microscopy—We used video-enhanced contrast, differential interference contrast microscopy (38) to follow MT dynamics as described below. Chambers with a volume of 3 μl were used. Two strips of double-sided tape were fixed on a microscope slide (Select Micro Slide, 76 × 22 mm, 0.8 mm thick, Chance Propper Ltd, United Kingdom; catalog number BS3836–1975) approximately 3 mm apart and perpendicular to the long axis of the slide. A 22 × 22-mm coverslip (Gold Seal cover glass, Clay Adams, United Kingdom; catalog number 3306) was then placed on top of the two tape strips and firmly pressed to attach it well. Slide and coverslip were ethanol- and water-washed prior to use. The channel formed by the tape strips, the slide, and the coverslip made up the chamber. Prior to use, centrosomes (3×10^3/μl) with a working concentration of tubulin in BRB80 (80 mM K-Pipes, 1 mM EGTA, 1 mM $MgCl_2$) were injected into the chamber and left for 5 min on ice. The sample (always 30-μl total volume) was mixed on ice and consisted of BRB80, 1 mM GTP, tubulin, and stathmin or control buffer (the sample contained 1 μl of control buffer or 1 μl of concentrated stathmin (30-fold dilution)). Using a paper towel and capillary forces, the 30-μl sample was flowed through the chamber, which was then sealed at both ends with grease, and placed on the stage of a Zeiss Axioskop (Zeiss GmbH, Oberkochen, Germany), equipped with a Zeiss × 100 Achrostigmat × 100/1.25 oil objective and a Hamamatsu Phototonics (Japan) C3077 CCD camera. Objective and condenser were heated to 37 °C, and the temperature inside the chamber was 37 °C (measured with a thermocouple). Measurements of MT dynamics were performed as described previously (39) using NIH 1.617b and Microsoft Excel 5 programs. No sample was observed for more than 40 min.

Sedimentation Velocity—Sedimentation velocity experiments were performed at 20 °C in a Beckman Optima XL-A ultracentrifuge equipped with a Ti60 titanium four-hole rotor with two-channel 12-mm path length centerpieces. Sample volumes of 400 μl were centrifuged at 45,000 rpm, and radial scans were taken at 280 nm at 5-min intervals. At this wavelength, tubulin is the only species detected, since the extinction coefficient of stathmin is very low due to its lack of aromatic residues. Data analysis was performed using the program dc/dt (40). The partial specific volume of the complex was estimated to be 0.73 ml/g, the solvent density taken as 1.005 g/cm^3, and its viscosity as 1.002 centipoise.

Gel Electrophoresis and Western Blots—One-dimensional electrophoresis was performed on 13% SDS-polyacrylamide gels (41). Proteins were either silver-stained on fixed gels as described previously (2) or immunoblotted as follows. Proteins were transferred onto 0.2-μm nitrocellulose filters (Schleicher & Schuell, Germany) in a semidry electroblotting apparatus (transfer buffer: 48 mM Tris, 39 mM glycine, 20% isopropyl alcohol). The membrane was saturated with 5% nonfat dry milk in immunoblot solution (12 mM Tris-HCl, pH 7.4, 160 mM NaCl, 0.1% Triton X-100). Membranes were probed with the stathmin antiserum directed against its C-terminal peptide (7) at 1:5000 dilution and a mouse monoclonal antibody against α-tubulin (N356, Amersham, UK) at 1:3000 dilution. Bound antibodies were detected by chemiluminescence (ECL, Amersham, UK) with the appropriate secondary antibodies and the membranes were exposed to XAR5 film (Eastman Kodak Co.).

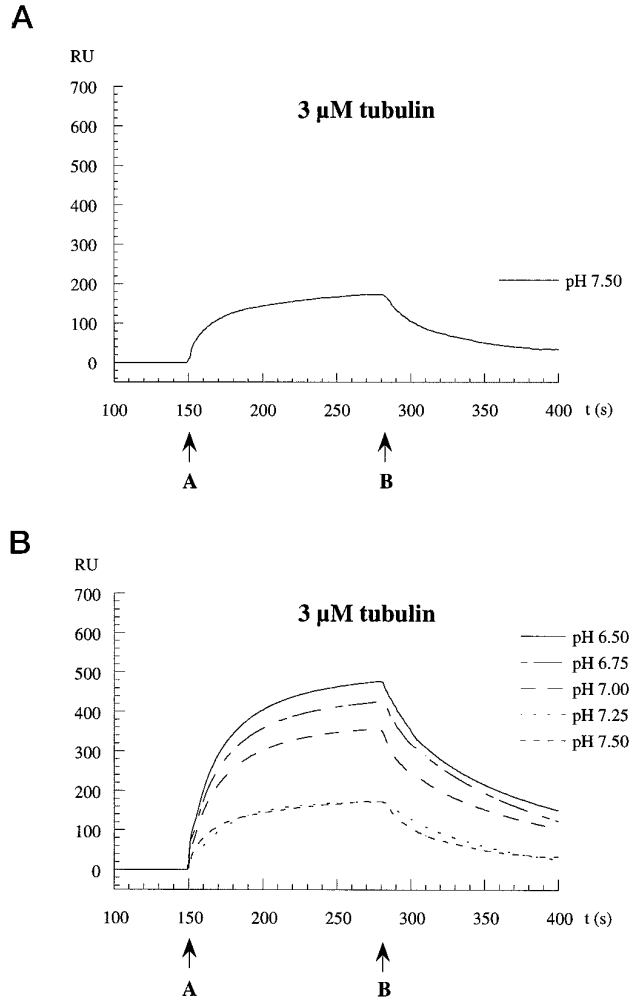

FIG. 1. **Plasmon resonance monitoring of tubulin interaction with stathmin surface.** *A*, net sensorgram (relative response in RU after background subtraction *versus* time in seconds) of tubulin injected over WT stathmin surface at a flow rate of 7 μl/min in buffer AB, pH 7.5. Injection of 3 μM tubulin started at *point A* and ended at *point B*. The interaction between tubulin and stathmin is indicated by the increase of the bound response units during the injection of protein. For background correction, we subtracted the signal obtained with a control flow cell coupled with BSA and injected with the same sample. *B*, net sensorgrams showing injection of 3 μM tubulin diluted in AB buffer at varying pH over the same WT stathmin surface as in *panel A*. Affinities, reflected by maximal binding levels, increased with the lower pH values.

For the determination of the stoichiometry of the stathmin-tubulin complex, samples of unknown concentration were compared with stathmin and tubulin standards whose concentrations were determined by amino acid analysis. The blots were probed with rabbit stathmin antiserum at 1:5000 dilution mixed, respectively, with either mouse monoclonal antibodies against α-tubulin or β-tubulin at 1:3000 dilution (N356 and N357, respectively, Amersham, UK). Appropriate secondary antibodies used were ^{35}S-labeled whole antibody to rabbit Ig (SJ434, Amersham, UK) and ^{35}S-labeled whole antibody to mouse Ig (SJ431, Amersham, UK). Quantification of stathmin, α-tubulin, or β-tubulin was achieved by direct counting of the radioactivity in each relevant ^{35}S-labeled band with an Instant Imager apparatus (Packard Instruments, Meriden, CT).

RESULTS AND DISCUSSION

Stathmin Interacts Directly with Tubulin—The stathmin/tubulin interaction was revealed by using the plasmon resonance technology. This method allows a real time observation of binding of molecules to surface immobilized ligands with no need to label either of the two (42). Mass variations in the vicinity of the surface are detected. Upon the addition of a molecule in solution to a surface bound ligand, the signal measured, which is proportional to the mass detected, provides a sensorgram, which allows to monitor the interaction.

Fig. 1*A* shows the net binding of pure tubulin to immobilized WT stathmin. 3 μM tubulin in AB buffer, pH 7.5, was injected at point A, and the injection was terminated at point B when the buffer was allowed to flow over the sensor surface. We then varied the pH of the buffer to screen for the best conditions of this interaction. Fig. 1*B* shows an overlay plot of net interaction curves obtained with 3 μM tubulin injected in AB buffer at pH varying between 7.5 and 6.5, with 0.25 pH unit steps. Comparison of the binding curves allowed us to evaluate the effect of pH on the affinity of the stathmin/tubulin interaction; the higher the steady state level, the higher the affinity (42). It was of the same order at pH 7.5 or 7.25 and rose sharply at pH 7 or below, being maximal at pH 6.5. The affinity dramatically fell at lower pH (not shown). All the following experiments were therefore performed in buffer AB at pH 6.5.

The specificity of the interaction was ascertained by the absence of tubulin binding to flow cells coupled with BSA (Fig. 2*A*) or simply activated-deactivated (not shown), the reduction of binding in buffer without Mg^{2+} (Fig. 2*B*), and the possibility of competing for tubulin binding to the surface immobilized stathmin by adding soluble stathmin to the tubulin solution prior to injection (Fig. 2*C*). Furthermore, this competition assay showed that tubulin binding to immobilized stathmin was abolished when 2 μM stathmin was added to a 4 μM tubulin flowing solution. This latter result suggested that at these stathmin and tubulin concentrations, more than 90% of the tubulin was complexed with stathmin in the solution, indicating that the solution K_D is at least 1 order of magnitude below this concentration range.

Affinity Determination from Kinetic Measurements—Buffer AB, pH 6.5, was used throughout this study. Interaction of tubulin with immobilized stathmin was studied over a tubulin concentration range of 1–20 μM. Fig. 3 shows representative net sensorgrams of association, steady state binding, and dissociation using various tubulin concentrations. For the determination of the dissociation rate constant, k'_d, rebinding of any released tubulin to the immobilized stathmin was prevented by raising the flow rate to 100 μl/min at the end of injection (*point B*). The dissociation phase was fitted according to the model $AB = A + B$, assuming a single site interaction between stathmin and tubulin. k'_d was equal to $5 \pm 0.15 \times 10^{-3}$ s^{-1} as calculated by fitting the data to Equation 2 (see "Experimental Procedures"). An association constant k'_a was then obtained by fitting the association phase with Equation 3 and was equal to $8.9 \pm 1 \times 10^3$ M^{-1} s^{-1}. The equilibrium dissociation constant k'_D was then calculated as k'_d/k'_a and was found to be $0.56 \pm 0.05 \times 10^{-6}$ M. A k'_D in the micromolar range reflects a relatively low affinity for the stathmin/tubulin interaction. This low affinity is in agreement with our earlier attempts in solution where we failed to retain tubulin by affinity onto a stathmin-Sepharose column or to co-immunoprecipitate tubulin with stathmin-antistathmin-protein A-Sepharose beads.[2] Furthermore, this relatively low affinity is in agreement with the intracellular concentration of tubulin in the cell also found in the micromolar range and gives weight to the idea that this stathmin/tubulin interaction is of physiological relevance (43).

Rate constants were found similar to those measured with WT stathmin when the sensor chip was coupled with bWT, with an unphosphorylatable form of stathmin (4A), or with a series of "pseudophosphorylated" stathmin mutants aimed to mimic stathmin phosphorylated by Ca^{2+}/calmodulin-depend-

[2] P. Curmi and V. Manceau, unpublished data.

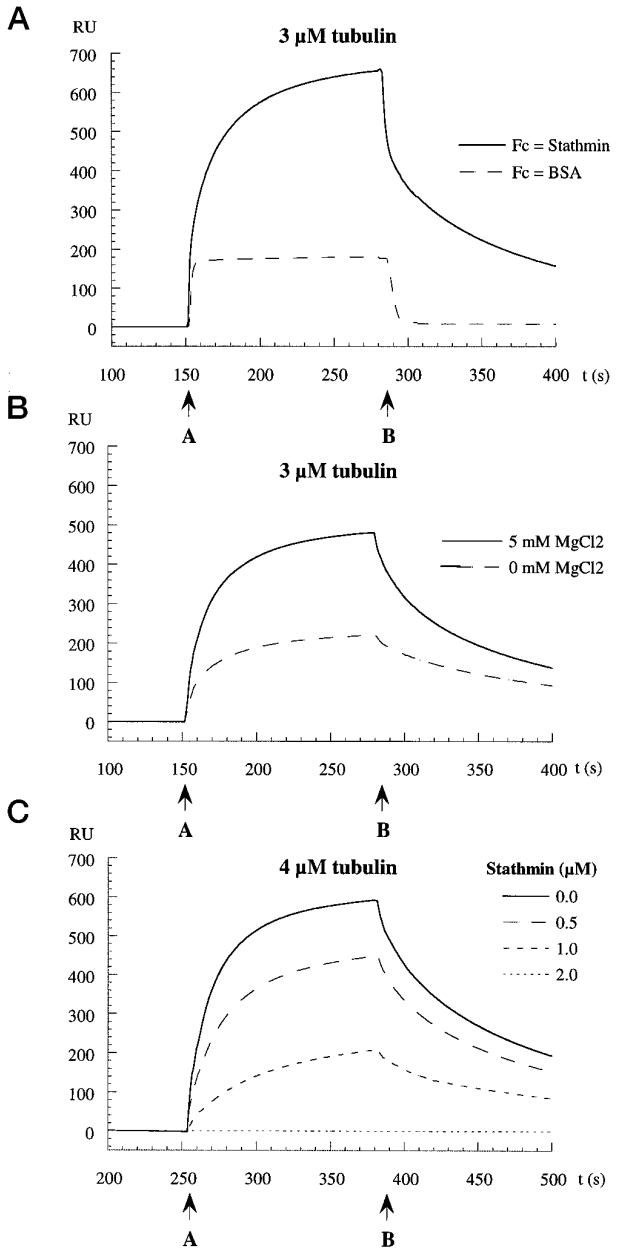

FIG. 2. **Specificity of the stathmin tubulin interaction.** *A*, sensorgrams showing injection of 3 μM tubulin in AB buffer, pH 6.5, over the WT stathmin and BSA control Fc. Sensorgrams demonstrate the specificity of tubulin binding to the stathmin Fc; changes in the signal observed with the BSA Fc were due to protein affecting the bulk refractive index of the running buffer. These large changes are also observed at the start and end of injection over the stathmin Fc and are subtracted as background in the net sensorgrams. *B*, net sensorgrams showing injection of 3 μM tubulin over the WT stathmin Fc in AB buffer, pH 6.5, with or without 5 mM $MgCl_2$. Specificity of the interaction is evidenced by the reduction of binding observed in the absence of $MgCl_2$. *C*, net sensorgrams showing injection of 4 μM tubulin over the WT stathmin Fc in AB buffer, pH 6.5, preincubated (5 min, room temperature) or not preincubated with competing concentrations of stathmin in solution. A dose-dependent reduction of surface binding was observed with increasing concentrations of stathmin. Surface binding was totally abolished when tubulin was preincubated with 2 μM stathmin, suggesting a two stathmin-one tubulin heterodimer complex in the flowing solution. On each *curve*, the start and end of injections of proteins are indicated with *arrows A* and *B*, respectively.

ent kinase II or IV on serine 16 (16E), by mitogen-activated protein kinase on serine 25 (25E), by Cdc2 kinase on serine 38 (38E), or by mitogen-activated protein kinase and Cdc2 on serines 25 and 38 (25/38E).

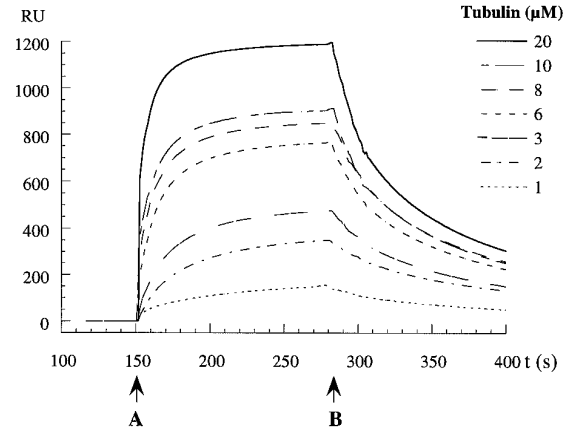

FIG. 3. **Plasmon resonance kinetic analysis of tubulin binding to WT stathmin surface.** Representative net sensorgrams illustrating the real time binding of tubulin to WT stathmin immobilized on the sensor chip at various tubulin concentrations. *A* indicates the start of association by injecting tubulin in AB buffer, pH 6.5. *B* indicates the start of dissociation by changing to buffer AB, pH 6.5, containing no tubulin. Analyses were performed as described under "Experimental Procedures." k'_d was $5 \pm 0.15 \times 10^{-3}$ s^{-1}, k'_a was $8.9 \pm 1 \times 10^3$ M^{-1} s^{-1}, and k'_D calculated as k'_d/k'_a was $0.56 \pm 0.05 \times 10^{-6}$ M.

On the other hand, when the sensor chip was coupled with the fully pseudophosphorylated 4E mutated stathmin (where all four phosphorylation sites of stathmin were replaced by Glu), k'_d and k'_a were $8 \pm 0.1 \times 10^{-3}$ s^{-1} and $5 \pm 0.1 \times 10^3$ M^{-1} s^{-1}, respectively, leading to a calculated k'_D of $1.6 \pm 0.2 \times 10^{-6}$ M. This result corresponds to about a 3-fold lowered affinity of 4E stathmin as compared with WT stathmin. Horwitz *et al.* (33) observed no difference between WT and a 4D mutant of stathmin (where the four serines were replaced by Asp) in their ability to inhibit polymerization or elicit depolymerization of MTs *in vitro*. This may be due to the relatively modest difference in k'_D between WT and 4E (and probably 4D mutants). However, it is likely that differences in k'_D may be more important at other working pH levels or different ionic conditions from those existing in the cell, since we observed in our preliminary attempts that at pH 7.5 no binding of tubulin was observed on a 4E-coupled sensor chip surface. It thus appears that a direct modulation of the stathmin/tubulin interaction may be the consequence of stathmin phosphorylation. Our result is indeed in agreement with that of Melander Gradin *et al.* (44), who recently showed with a cross-linking procedure that stathmin, immunopurified from K562 cells, interacts with tubulin, while this interaction was dramatically reduced when a mixture of stathmin phosphoforms was immunopurified from cells transfected with a constitutively active mutant of Ca^{2+}/calmodulin-dependent kinase IV/Gr. This modulation may explain the absence of MT destabilization observed with pseudophosphorylated stathmin mutants *in vivo* and is possibly due to a conformational change of stathmin upon phosphorylation modifying the accessibility of its C-terminal interaction domain without the need of a third intervening protein partner as suggested by Horwitz *et al.* (33).

Stathmin and Tubulin form a 60-Å Stokes Radius Complex—The Stokes radius of the stathmin-tubulin complex was determined by gel filtration chromatography. Pure stathmin and pure tubulin were applied separately or immediately after mixing to a column equilibrated with AB buffer, pH 6.5, at room temperature. Tubulin and stathmin-tubulin complex elutions were monitored at 280 nm with no interference of free stathmin, since it absorbs very poorly at 280 nm due to the lack of aromatic residues. Fig. 4 shows representative elution profiles for pure tubulin or tubulin mixed with WT stathmin. Pure

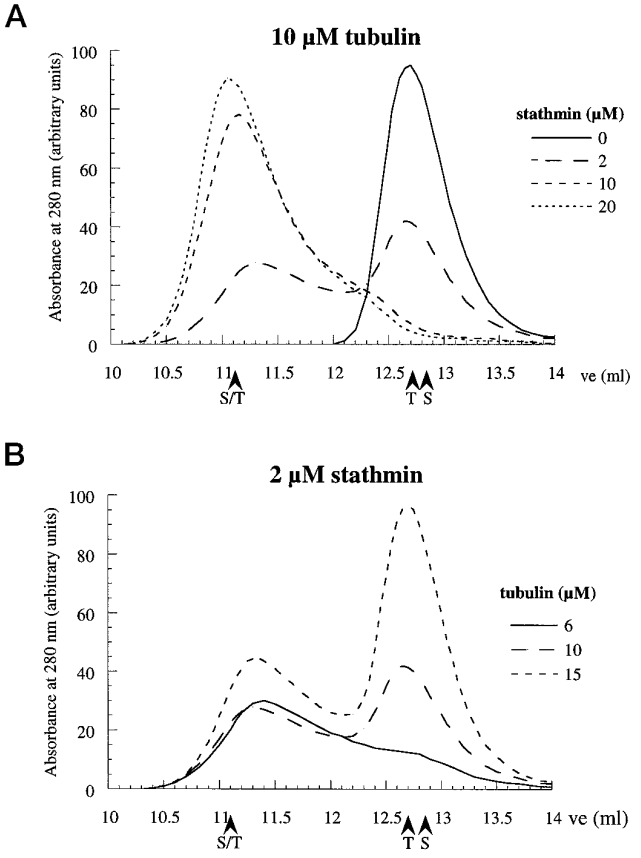

FIG. 4. **Gel filtration analysis of tubulin and of the stathmin-tubulin complex.** Representative FPLC elution profiles are shown of tubulin and of the stathmin-tubulin complex applied at room temperature to a Superose-12 HR 10/30 gel filtration column equilibrated with AB buffer, pH 6.5. Records were achieved at 280 nm, since at this wavelength only tubulin causes absorbance. 100-μl samples containing 10 μM tubulin alone or 10 μM tubulin premixed with 2, 10, or 20 μM stathmin for 5 min at room temperature (*A*) or 2 μM stathmin premixed for 5 min at room temperature, with 6, 10, or 15 μM tubulin (*B*) were applied to the column. Elution was performed with the same buffer. *Arrow S* indicates the elution volume of the stathmin peak as determined by Western blotting (Fig. 5), and *arrow T* indicates the elution volume of the tubulin peak observed in the absence of stathmin. The mixture of stathmin with tubulin provoked a variable shift of the tubulin peak toward a mean minimum elution volume value of 11.1 ± 0.1 ml (*arrow S/T*). The shifted peaks correspond to the stathmin-tubulin complex as evidenced by Western blotting (Fig. 5). Intermediate peaks reflected dissociation of stathmin-tubulin complexes.

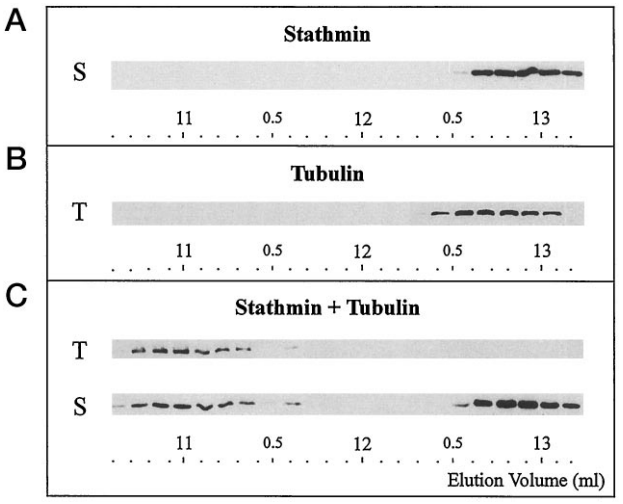

FIG. 5. **Interaction between stathmin and tubulin evidenced by gel filtration chromatography.** Western blot analyses of stathmin, tubulin, and stathmin-tubulin were applied to a FPLC Superose 12 HR 10/30 gel filtration column equilibrated with AB buffer, pH 6.5 as in Fig. 4. Elution was performed with the same buffer, and fractions of 80 μl each were collected. *A*, a 20 μM stathmin sample was applied to the column. Elution volume of the stathmin peak was evaluated at 12.8–12.9 ml. *B*, a 10 μM tubulin sample was applied to the column. Elution volume of the tubulin peak was found at 12.7 ± 0.1 ml. *C*, a sample containing 20 μM stathmin premixed with 10 μM tubulin was applied to the column. Two peaks were observed, a peak eluting at ~11 ml, representing the stathmin-tubulin complex, and a residual stathmin peak at ~12.8 ml. Note the small intermediate stathmin-tubulin peak at ~ 11.6 ml due to a partial dissociation of the stathmin-tubulin complex.

tubulin eluted at about 12.7 ± 0.1 ml. The addition of stathmin provoked a variable shift of the tubulin peak toward a minimum value of the elution volume of about 11.1 ± 0.1 ml. This shifted peak, as analyzed by one-dimensional Western blotting was always composed of stathmin and tubulin and thus represented the stathmin-tubulin complex (Fig. 5). The relative importance of the shift and intensity of the shifted peak were dependent both on the absolute concentrations of tubulin and stathmin and on the molar ratio of the two proteins in the loaded sample, as demonstrated by the elution profiles obtained with 10 μM tubulin and variable amounts of stathmin (Fig. 4*A*) and with 2 μM stathmin and variable amounts of tubulin (Fig. 4*B*). To better analyze the conditions of the stathmin/tubulin interaction, we plotted (Fig. 6) the molecular sieve coefficient, K_{av} $((V_e - V_0)/(V_t - V_0)$; see "Experimental Procedures") of the shifted peak *versus* protein concentration. Shifts reached a K_{av} plateau of 0.26–0.27 above a concentration of 2 μM stathmin for 10 μM tubulin (Fig. 6*A*). Values observed with stathmin concentrations under the threshold of 2 μM stathmin for 10 μM tubulin were most probably due to dissociation of the complex during the run, since the morphology of the peak was clearly asymmetrical in these conditions (see Fig. 4). Similarly, we found that K_{av} reached a plateau of comparable value over a 5 μM tubulin to 2 μM stathmin ratio (Fig. 6*B*). The stoichiometry was not directly accessible from the analysis of these curves, since a variable amount of tubulin aggregated and migrated in the void volume, apparently without associated stathmin as assessed by one-dimensional Western blotting. We thus determined directly by Western blotting the stathmin tubulin stoichiometry of the complex in peak fractions collected at the K_{av} plateau (see "Experimental Procedures"). A stoichiometry of one stathmin for two tubulin $\alpha\beta$-heterodimers was steadily measured through the K_{av} plateau (Table I), indicating the formation of a 217-kDa (calculated value) molecular complex.

The Stokes radius of the complex was determined by reporting minimal K_{av} values of the stathmin-tubulin complex peak on a $(-\log K_{av})^{1/2}$ *versus* Stokes radius graph constructed with a series of reference proteins. The Stokes radius of stathmin was 37 Å, slightly different from the value of 33 Å found with the native bovine brain protein (45) and that of tubulin (41.5 Å), and the Stokes radius of the stathmin-tubulin complex was 60 ± 1 Å (Fig. 7). The comparison of the calculated molecular weight of the one stathmin-two tubulin complex to that of a globular 60-Å protein (about 430 kDa), indicates that the stathmin-tubulin complex presents an asymmetrical conformation.

Sedimentation Analysis—Sedimentation velocity experiments were performed to assess the sample heterogeneity as well as to measure directly the molecular weights of stathmin, tubulin, and the complex in the native state. All experiments were performed in AB buffer, pH 6.5. The sedimentation of tubulin was found to be 5.66 S in these conditions, as reported (46). When tubulin and stathmin were mixed at respective concentrations of 10 and 20 μM, so that all tubulin would be complexed to stathmin, a single symmetrical boundary of tu-

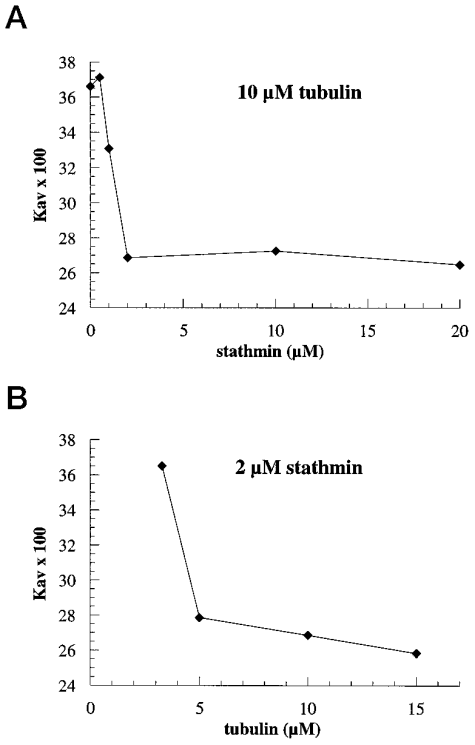

FIG. 6. **K_{av} of tubulin and of the stathmin-tubulin complex.** K_{av} values were determined from elution positions of the shifted peak observed with 10 μM tubulin or 10 μM tubulin premixed with various concentrations of stathmin upon FPLC chromatography on a Superose 12 HR 10/30 gel filtration column (*A*). K_{av} reached a plateau over a stathmin:tubulin molar ratio of about 2/10. *B*, 2 μM stathmin was mixed with varying concentrations of tubulin. A K_{av} plateau was observed for a stathmin:tubulin molar ratio of about 2:5.

TABLE I
Direct determination of the stoichiometry of the stathmin-tubulin complex

Molar concentrations of stathmin (S), α-tubulin (α-T) and β-tubulin (β-T) were determined by quantitative Western blotting (as described under "Experimental Procedures") in stathmin-tubulin complexes isolated by gel filtration chromatography. Gel filtration runs were performed with 10 μM tubulin mixed to 2 (experiment I), 10 (experiment II) and 20 (experiment III) μM stathmin, respectively, and the fractions analyzed were collected at the beginning (a), middle (b), and at the top (c) of the ascending slope of the stathmin-tubulin complex peak. A mean tubulin:stathmin molar ratio of about 2 was found with both α- and β-tubulin throughout the K_{av} plateau (see Fig. 6).

		Tubulin:stathmin molar ratio	
		[α-T]/S	[β-T]/S
Exp I	a	2.13	1.78
	b	2.30	1.85
	c	1.87	2.10
Exp. II	a	1.90	2.06
	b	2.23	1.80
	c	1.75	2.27
Exp. III	a	1.80	2.17
	b	2.27	1.87
	c	1.97	2.08
	Mean	2.02	1.99
	S.D.	0.20	0.16

bulin-containing species was observed; the data could be fitted with a species sedimenting at 7.7 S and accounting for more than 98% of the total tubulin. Taking into account our evaluation of the Stokes radius, the molecular mass of the corresponding complex can be calculated from the Svedberg equation (47) to be 197 kDa, which, given the uncertainties of the Stokes radius and of other physical constants, is consistent with the calculated mass (217 kDa) for a one stathmin-two tubulin $\alpha\beta$-heterodimer complex.

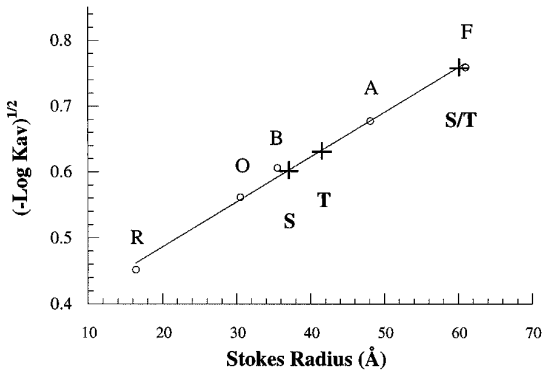

FIG. 7. **The stathmin-tubulin complex has a 60-Å Stokes radius.** A Superose 12 HR 10/30 FPLC gel filtration column was calibrated by using a series of standard proteins: ribonuclease A (*R*), ovalbumin (*O*), bovine serum albumin (*B*), aldolase (*A*), and ferritin (*F*). Upon gel filtration, a linear relationship ($y = 0.35 + 6.8 \times 10^{-3}x$, $r = 0.99$) was noted between the Stokes radii of standard proteins and $(-\log K_{av})^{1/2}$ (○). Stokes radii of stathmin (*S*), tubulin (*T*), and the stathmin-tubulin complex (*S*/*T*) were then determined graphically and found to be 37, 41.5, and 60 Å, respectively (+).

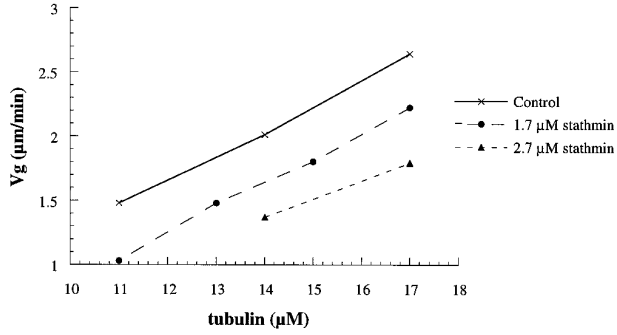

FIG. 8. **Stathmin reduces the growth rate of microtubules.** We used video-enhanced contrast, differential interference contrast microscopy to follow MT dynamics. The experiments were performed in a chamber at 37 °C with BRB80 plus 1 mM GTP (see "Experimental Procedures"). MTs were analyzed during growth off centrosomes in the absence or presence of stathmin. The addition of stathmin resulted in a dose-dependent reduction of Vg. Moreover, curves relating Vg to tubulin concentration were found parallel in the presence or absence of stathmin, suggesting that stathmin sequesters free tubulin heterodimers.

Stathmin Impedance of Microtubule Growth May Be Partly Due to Tubulin Sequestration in the Stathmin-Tubulin Complex—The effect of stathmin on MT dynamics was investigated on centrosome-nucleated MTs by video microscopy (39, 48). Tubulin concentrations in this study varied between 11 and 17 μM where MTs grew at a rate (Vg) of 1.48–2.64 μm/min, respectively (Fig. 8 and Table II). The number of catastrophes was low and varied between 0 and 4 in these conditions, which led to a catastrophe frequency (f_{cat}) of 0–0.039 min^{-1}. As evidenced on Fig. 8, the addition of stathmin resulted in a reduction of Vg. Moreover, the Vg dependence on tubulin concentration observed in the presence of two different stathmin concentrations was parallel to that observed in the absence of stathmin.

At Vg = 1.5 μm/min, the displacement of the curves by 1.7 and 2.7 μM stathmin corresponds to 2 and 3.8 μM tubulin, respectively. If the curve displacement reflects a sequestration of tubulin by its interaction with stathmin, these results would indicate a 1:1.2 and 1:1.4 stathmin:tubulin heterodimer molar ratio. This result is not identical with but fits the stoichiometry determined by immunodetection after chromatography. It is therefore most likely that stathmin indeed influences MT

TABLE II

Stathmin reduces Vg and does not alter the catastrophe frequency

MT dynamics was followed with video-enhanced contrast, differential interference contrast microscopy (see "Experimental Procedures"). The tubulin and stathmin concentrations inside the video chamber are indicated. In the experiments concerning f_{cat}, MTs grown at the same growth rate in the presence or absence of stathmin were compared, and the f_{cat} values were obtained for the indicated total time.

	Tubulin				
	11 μM	13 μM	14 μM	15 μM	17 μM
No stathmin					
Vg[a]	1.48 ± 0.59	ND[b]	2.01 ± 0.58	ND	2.64 ± 0.49
f_{cat}	0.039	ND	0.039	ND	0
d	25	ND	14	ND	13
e	84	ND	47	ND	55
f	102	ND	50	ND	45
g	4	ND	2	ND	0
1.7 μM stathmin					
Vg	1.03 ± 0.85	1.48 ± 0.40	ND	1.8 ± 0.90	2.22 ± 0.52
f_{cat}	0.18	0.02	ND	0.028	0
d	6	12	ND	14	15
e	22	30	ND	32	47
f	17	47	ND	36	44
g	3	1	ND	1	0
2.7 μM stathmin					
Vg	NP[h]	ND	1.37 ± 0.76	ND	1.79 ± 0.60
f_{cat}	NP	ND	0.077	ND	0.029
d	NP	ND	12	ND	16
e	NP	ND	48	ND	69
f	NP	ND	52	ND	69
g	NP	ND	4	ND	2

[a] Vg, growth rate ± S.D. (μm/min).
[b] ND,not determined.
[c] f_{cat}, catastrophes/min.
[d] Number of MT measured.
[e] Number of individual measurements.
[f] Total time of observation (min).
[g] Number of catastrophes.
[h] NP, no polymerization.

growth by sequestering tubulin heterodimers. However, the effect of stathmin on MT polymerization may be not simply due to tubulin sequestration, since at 11 μM tubulin and 2.7 μM stathmin, no polymerization occurred, whereas simple curve extrapolation should have led to a significant residual polymerization level. This may reflect an additional nonlinear component in the effect of stathmin on MT polymerization.

Importantly, we found that at similar Vg, f_{cat} was unchanged in presence of stathmin (Table II). Our result is clearly different from that reported by Belmont and Mitchison (30), who found in a similar assay that the catastrophe rate is 5–10-fold higher in the presence of stathmin. This might be an important point still to be investigated, since in our study the sequestration of tubulin by stathmin in a stathmin-tubulin complex, by reducing the available tubulin concentration, seems to account for a large part to the reduction of net MT polymerization. Reasons for this divergence are not clear. Part of it may be explained by differences in the source of the protein or in the buffers used in the two studies, possibly conditioning the dynamic instability of MTs. Belmont and Mitchison (30) used purified stathmin from *calf* in a pH 7.5 buffer containing 5 mM $MgCl_2$, whereas our study was performed with recombinant human stathmin in BRB80 buffer, pH 6.8, the reference buffer for studies on MT dynamics *in vitro*.

Conclusion—We have demonstrated in the present work that a direct interaction between stathmin and tubulin occurs *in vitro* and gives rise to a complex formed by one stathmin molecule and two tubulin αβ-heterodimers. The stathmin/tubulin interaction has a k'_D of about 0.5 μM and is sensitive to ionic variations; it occurs preferentially at an optimum pH of about 6.5. We found that the 4E pseudophosphorylated mutant of stathmin has an altered affinity for tubulin *in vitro*, which may indicate that, *in vivo*, stathmin phosphorylation directly regulates the stathmin/tubulin interaction without intervening protein partners. Our results further indicate that one of the mechanisms of the stathmin destabilization of MTs might be the sequestration of free tubulin heterodimers in a stathmin-tubulin complex.

Acknowledgments—We thank G. Batelier from Laboratoire d'Enzymologie et Biologie Structurale UPR9063 CNRS, Gif sur Yvette, France, for help in performing the ultracentrifugation experiments, M. Dutreix from the Institut Curie, Paris, France, for skillful help in performing the BIAcore experiments, and M. F. Carlier for critical reading of this manuscript.

REFERENCES

1. Sobel, A. (1991) *Trends Biochem. Sci.* **16,** 301–305
2. Sobel, A., Boutterin, M.-C., Beretta, L., Chneiweiss, H., Doye, V., and Peyro-Saint-Paul, H. (1989) *J. Biol. Chem.* **264,** 3765–3772
3. Pasmantier, R., Danoff, A., Fleischer, N., and Schubart, U. K. (1986) *Endocrinology* **19,** 1229–1238
4. Schubart, U. K., Yu, J. H., Amat, J. A., Wang, Z. Q., Hoffmann, M. K., and Edelmann, W. (1996) *J. Biol. Chem.* **271,** 14062–14066
5. Hailat, N., Strahler, J. R., Melhem, R. F., Zhu, X. X., Brodeur, G., Seeger, R. C., Reynolds, C. P., and Hanash, S. M. (1990) *Oncogene* **5,** 1615–1618
6. Cooper, H. L., Fuldner, R., McDuffie, E., and Braverman, R. (1991) *J. Immunol.* **146,** 3689–3696
7. Koppel, J., Boutterin, M.-C., Doye, V., Peyro-Saint-Paul, H., and Sobel, A. (1990) *J. Biol. Chem.* **265,** 3703–3707
8. Maucuer, A., Moreau, J., Mechali, M., and Sobel, A. (1993) *J. Biol. Chem.* **268,** 16420–16429
9. Chneiweiss, H., Beretta, L., Cordier, J., Boutterin, M. C., Glowinski, J., and Sobel, A. (1989) *J. Neurochem.* **53,** 856–863
10. Amat, J. A., Fields, K. L., and Schubart, U. K. (1991) *Dev. Brain Res.* **60,** 205–218
11. Peschanski, M., Doye, V., Hirsch, E., Marty, L., Dusart, I., Manceau, V., and Sobel, A. (1993) *J. Comp. Neurol.* **337,** 655–668
12. Schubart, U. K. (1988) *J. Biol. Chem.* **263,** 12156–12160
13. Doye, V., Kellermann, O., Buc-Caron, M. H., and Sobel, A. (1992) *Differentiation* **50,** 89–96
14. Pampfer, S., Fan, W., Schubart, U. K., and Pollard, J. W. (1992) *Reprod. Fertil. Dev.* **4,** 205–211
15. Koppel, J., Loyer, P., Maucuer, A., Rehák, P., Manceau, V., Guguen-Guillouzo, C., and Sobel, A. (1993) *FEBS Lett.* **331,** 65–70
16. Okazaki, T., Himi, T., Peterson, C., and Mori, N. (1993) *FEBS Lett.* **336,** 8–12
17. Balogh, A., Mege, R. M., and Sobel, A. (1996) *Exp. Cell Res.* **224,** 8–15
18. Hanash, S. M., Strahler, J. R., Kuick, R., Chu, E. H. Y., and Nichols, D. (1988) *J. Biol. Chem.* **263,** 12813–12815
19. Friedrich, B., Grönberg, H., Landström, M., Bergh, A., and Gullberg, M. (1995) *Prostate* **27,** 102–109

20. Beretta, L., Boutterin, M.-C., and Sobel, A. (1988) *Endocrinology* **122,** 40–51
21. le Gouvello, S., Chneiweiss, H., Tarantino, M., Debré, P., and Sobel, A. (1991) *FEBS Lett.* **287,** 80–84
22. Chneiweiss, H., Cordier, J., and Sobel, A. (1992) *J. Neurochem.* **58,** 282–289
23. Doye, V., Boutterin, M.-C., and Sobel, A. (1990) *J. Biol. Chem.* **265,** 11650–11655
24. Larsson, N., Melander, H., Marklund, U., Osterman, O., and Gullberg, M. (1995) *J. Biol. Chem.* **270,** 14175–14183
25. Marklund, U., Osterman, O., Melander, H., Bergh, A., and Gullberg, M. (1994) *J. Biol. Chem.* **269,** 30626–30635
26. Ozon, S., Maucuer, A., and Sobel, A. (1997) *Eur. J. Biochem.* **248,** in press
27. Beretta, L., Dobransky, T., and Sobel, A. (1993) *J. Biol. Chem.* **268,** 20076–20084
28. Maucuer, A., Camonis, J. H., and Sobel, A. (1995) *Proc. Natl. Acad. Sci. U. S. A.* **92,** 3100–3104
29. Maucuer, A., Ozon, S., Manceau, V., Gavet, O., Lawler, S., Curmi, P., and Sobel, A. (1997) *J. Biol. Chem.* **272,** 455712
30. Belmont, L. D., and Mitchison, T. J. (1996) *Cell* **84,** 623–631
31. Walczak, C. E., Mitchison, T. J., and Desai, A. (1996) *Cell* **84,** 37–47
32. Marklund, U., Larsson, N., Melander Gradin, H., Brattsand, G., and Gullberg, M. (1996) *EMBO J.* **15,** 5290–5298
33. Horwitz, S. B., Shen, H.-J., He, L., Dittmar, P., Neef, R., Chen, J., and Schubart, U. K. (1997) *J. Biol. Chem.* **272,** 8129–8132
34. Riederer, B. M., Pellier, V., Antonsson, B., Di Paolo, G., Stimpson, S. A., Lütjens, R., Catsicas, S., and Grenningloh, G. (1997) *Proc. Natl. Acad. Sci. U. S. A.* **94,** 741–745
35. Mitchison, T. J., and Kirschner, M. (1984) *Nature* **312,** 237–242
36. Curmi, P., Maucuer, A., Asselin, S., Lecourtois, M., Chaffotte, A., Schmitter, J. M., and Sobel, A. (1994) *Biochem. J.* **300,** 331–338
37. Siegel, L. M., and Monty, K. J. (1966) *Biochem. Biophys. Acta* **112,** 346–362
38. Allen, R. D., Allen, N. S., and Travis, J. L. (1981) *Cell Motil. Cytoskeleton* **1,** 291–302
39. Andersen, S. S. L., Buendia, B., Dominguez, J. E., Sawyer, A., and Karsenti, E. (1994) *J. Cell Biol.* **127,** 1289–1299
40. Stafford, W. F. (1992) *Anal. Biochem.* **203,** 295–301
41. Sobel, A., and Tashjian, A. H., Jr. (1983) *J. Biol. Chem.* **258,** 10312–10324
42. Karlsson, R., Michaelsson, A., and Mattsson, L. (1991) *J. Immunol. Methods* **145,** 229–240
43. Northrup, S. H., and Erickson, H. P. (1992) *Proc. Natl. Acad. Sci. U. S. A.* **89,** 3338–3342
44. Melander Gradin, H., Marklund, U., Larsson, N., Chatila, T. A., and Gullberg, M. (1997) *Mol. Cell. Biol.* **17,** 3459–3467
45. Schubart, U. K., Alago, W., Jr., and Danoff, A. (1987) *J. Biol. Chem.* **262,** 11871–11877
46. Prakash, V., and Timasheff, S. N. (1997) *J. Mol. Biol.* **160,** 499–515
47. Cantor, C. R., and Schimmel, P. R. (1980) *Biophysical Chemistry*, pp. 605–607, W. H. Freeman, San Francisco
48. Walker, R. A., O'Brien, E. T., Pryer, N. K., Sobeiro, M. F., Voter, W. A., Erickson, H. P., and Salmon, E. D. (1988) *J. Cell Biol.* **107,** 1437–1448